JACS
JOURNAL OF THE AMERICAN CHEMICAL SOCIETY

Communication

pubs.acs.org/JACS

Inorganically Functionalized PbS–CdS Colloidal Nanocrystals: Integration into Amorphous Chalcogenide Glass and Luminescent Properties

Maksym V. Kovalenko,*[,†,⊥] Richard D. Schaller,[‡,§] Dorota Jarzab,[∥] Maria A. Loi,[∥] and Dmitri V. Talapin*[,†,‡]

[†]Department of Chemistry and James Franck Institute, University of Chicago, Chicago, Illinois 60637, United States
[‡]Center for Nanoscale Materials, Argonne National Laboratory, Argonne, Illinois 60439, United States
[§]Department of Chemistry, Northwestern University, Evanston, Illinois 60208, United States
[∥]Zernike Institute for Advanced Materials, University of Groningen, 9747 AG Groningen, The Netherlands

Supporting Information

ABSTRACT: Inorganic semiconductor nanocrystals (NCs) with bright, stable, and wavelength-tunable luminescence are very promising emitters for various photonic and optoelectronic applications. Recently developed strategies for inorganic surface capping of colloidal NCs using metal chalcogenide complexes have opened new perspectives for their applications. Here we report an all-inorganic surface functionalization of highly luminescent IR-emitting PbS–CdS NCs and studies of their luminescence properties. We show that inorganic capping allows simple low-temperature encapsulation of inorganic NCs into a solution-cast IR-transparent amorphous As_2S_3 matrix. The resulting all-inorganic thin films feature stable IR luminescence in the telecommunication wavelength region. The high optical dielectric constant of As_2S_3 also helps reduce the dielectric screening of the radiating field inside the quantum dot, enabling fast radiative recombination in PbS–CdS NCs.

Wet colloidal synthesis is known as a powerful methodology for producing highly monodisperse semiconductor nanocrystal (NC) quantum dots with superior optical properties.[1,2] In particular, the luminescence of II–VI, III–V, and IV–VI NCs covers the broad wavelength region from the UV through the visible and near-IR (NIR) while demonstrating very high quantum efficiencies and narrow emission spectra.[3−5] With excellent solution processability and high stability, semiconductor NCs represent some of the most promising materials for light-emitting devices and full color display technologies, with a strong potential for extension to the important NIR spectral region.[5−8]

It is well-known that surface chemistry and the surrounding medium exhibit a profound impact on the luminescent properties and stability of NCs. In particular, the development of stable and efficient NC-based IR emitters is hampered by transfer of the exciton energy to the molecular vibrational modes of organic ligands (mainly C–H stretches)[6,9] and to adjacent NCs. To address this problem, we present a novel solution-phase approach for preparing all-inorganic composite materials comprising IR-luminescent colloidal NCs embedded into an amorphous arsenic sulfide matrix (a-As_2S_3). Low-temperature solution casting allows deposition of such composites in the form of thin films on virtually any substrate. a-As_2S_3 is known as a low-loss optical waveguide material that is especially useful for IR applications. With an optical band gap of 2.25 eV,[10] As–S glasses are transparent from the NIR down to mid-IR cutoff wavelengths of ∼10 μm[11] while showing high refractive index (n = 2.4 at λ = 4.8 μm)[12] and good nonlinear optical properties. These features make As–S glasses an ideal host matrix for encapsulating IR-active NCs.

Our methodology for preparing NC/As_2S_3 composites is outlined in Figure 1. In the first step, oleate-capped PbS NCs

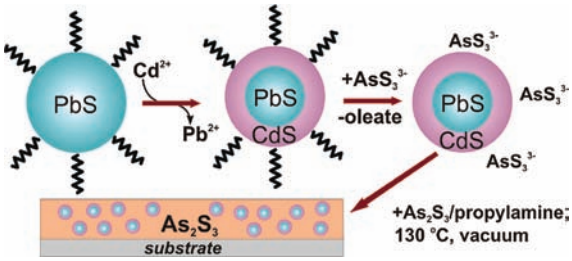

Figure 1. Schematics of the synthesis of all-inorganic IR-emitting colloidal PbS–CdS NCs and their low-temperature integration into an IR-transparent As_2S_3 chalcogenide glass matrix.

were subjected to a partial Pb-to-Cd cation-exchange reaction at 70–100 °C by adding a large excess of cadmium oleate (Cd:Pb ≈ 10:1), forming PbS–CdS core–shell NCs, similar to the general procedure reported by Pietryga et al.[13] The resulting 0.3–0.7 nm thick CdS shell (1–2 monolayers) provides chemical and electronic passivation of the PbS core, while the small lattice mismatch between CdS (zinc blende, a = 5.82 Å) and PbS (rock salt, a = 5.93 Å) ensures good crystallographic compatibility through sharing of a face-centered cubic sublattice of S atoms. Formation of the CdS shell was monitored by optical absorption spectroscopy

Received: September 16, 2011
Published: January 7, 2012

   dx.doi.org/10.1021/ja2087689 | J. Am. Chem.Soc. 2012, 134, 2457–2460

(Figures S1−S3 in the Supporting Information), which showed a significant shift of the excitonic peaks toward higher energies, and by powder X-ray diffraction (PXRD) (Figures S4 and S5), which indicated the change in average lattice constant; it was also confirmed by ICP−OES elemental analysis. The mean NC diameter estimated by transmission electron microscopy (Figure S6) did not change in the course of cation exchange. In the second step, the oleate capping of the PbS−CdS NCs was completely replaced with $(NH_4)_3AsS_3$ as a *thermally decomposable* ligand, similar to our previously reported procedures developed for various metal chalcogenide complexes (MCCs) as surface-capping ligands.[14] In the third step, we combined colloids of inorganically functionalized NCs with molecular solutions of a-As_2S_3 in propylamine (PA). The resulting homogeneous blend could be used for spin-coating of thin films. Mild thermal treatment of the composite films at 130 °C under vacuum nearly completely removed the organic material and converted the As−S precursors and $(NH_4)_3AsS_3$ into an a-As_2S_3 matrix.

The photoluminescence (PL) of the oleate-capped, inorganically functionalized PbS−CdS NCs spanned the entire NIR spectral region (Figure 2). The following discussion of optical

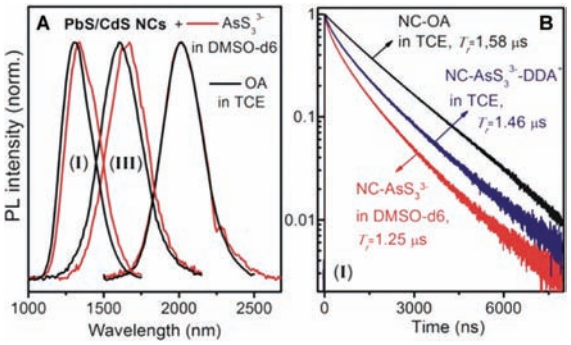

Figure 2. (A) PL spectra of oleate- and $(NH_4)_3AsS_3$-functionalized PbS−CdS NCs dispersed in IR-transparent solvents [tetrachloroethylene (TCE) and deuterated dimethyl sulfoxide (DMSO-d_6), respectively], covering the entire NIR spectral region. (B) PL decay kinetics for PbS−CdS NCs (sample **I**) with ∼4.2 nm PbS core and ∼0.3 nm CdS shell.

properties is focused on samples emitting in the 1000−1600 nm range (NC samples denoted as **I**, **II**, and **III**) because of the ease of steady-state and time-resolved PL measurements in this spectral region. At the same time, it is important to note that bright and stable PL was also observed at longer wavelengths of up to 2200 nm (Figure 2A) and from NCs with sub-2 nm cores emitting below 1000 nm (Figure S3).

In PbS−CdS heterostructures, a small conduction-band offset and a large valence-band offset[15] suggest that electron wave functions extend into the CdS shell while holes are efficiently confined in the PbS core, reducing the electron−hole overlap. Accordingly, oleate-capped PbS−CdS NCs exhibited nearly ideal monoexponential PL decays with higher PL quantum yields (QYs) and longer PL radiative lifetimes (T_r) than uncoated PbS NCs (T_r = 1.44 μs, QY = 29%): the T_r and QY were modestly improved for thin CdS shells (sample **I**, T_r = 1.58 μs, QY = 33.6%; Figure 1B) and significantly improved for thicker CdS shells (sample **II**, T_r = 2.4 μs, QY = 46.5%; Figure S2).

The key advantage of PbS−CdS NCs over PbS NCs is their much higher chemical stability and retention of bright PL through all of the processing steps outlined in Figure 1. The significant improvements in the chemical and photochemical stability of the NCs arose primarily from reduced surface trapping of holes. Similar to alkanethiols,[16] MCCs can be expected to act as hole traps. Accordingly, the PL of PbS NCs is significantly quenched (QY ≈ 1% or less) after the exchange with MCC ligands such as $(NH_4)_3AsS_3$ or $Na_4Sn_2S_6$. At the same time, only a modest decrease in the PL efficiency of PbS−CdS NCs was observed for $(NH_4)_3AsS_3$-stabilized PbS−CdS NCs in deuterated dimethyl sulfoxide [DMSO-d_6, which is transparent up to 2200 nm (Figure S7)], with typical QYs of ∼20% (20.3% for sample **I**, 19% for sample **II**). Electron delocalization onto inorganic ligands might explain the small 20−25 meV shift of the absorption and PL bands to longer wavelengths. In accord with the decreased QY, the PL decays became multiexponential because of the contribution from nonradiative processes. For consistent comparison of radiative lifetimes for all samples (liquid and solid), we used single-exponential fits to the longest-lived decay components (from 1000 ns onward) to get the best estimates; we found that T_r decreased only modestly (T_r = 1.25 μs for sample **I** in DMSO-d_6; Figure 2).

The ligand exchange with $(NH_4)_3AsS_3$ converted the sterically stabilized, oleate-capped NCs into charge-stabilized colloids. The disappearance of the IR absorption bands corresponding to the C−H stretching modes of the oleate surface ligands (2700−3000 cm^{-1}) was observed for AsS_3^{3-}-capped PbS−CdS NCs, confirming the completeness of the ligand exchange. The colloidal stability of the resulting solutions was evidenced by dynamic light scattering (DLS), which showed single-particle populations and smaller sizes relative to the original oleate-capped NCs (Figure 3A). The

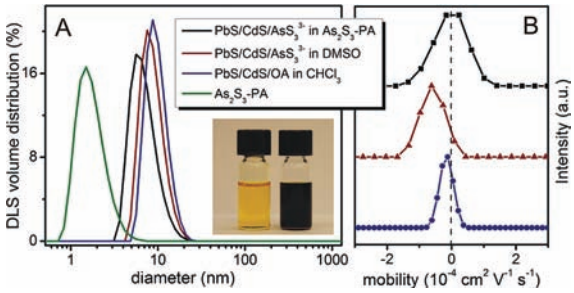

Figure 3. (A) DLS volume distributions and (B) electrophoretic mobilities of As_2S_3/propylamine (PA) solutions for ∼6.5 nm PbS−CdS NCs (sample **III**) before and after the ligand exchange and for a PbS−CdS/As_2S_3 mixture in PA. The inset shows As_2S_3/PA and PbS−CdS/As_2S_3/PA solutions.

electrostatic stabilization mechanism and negative surface charge were confirmed by electrophoretic mobility measurements (Figure 3B). The ζ potentials (calculated from Henry's equation in the Smoluchowski limit[17]) were −20 to −30 mV for AsS_3^{3-}-capped NCs in DMSO. The solubility of ion-capped NCs is largely determined by the solvent static dielectric constant ε. We found good solubility (20−100 mg/mL) of AsS_3^{3-}-capped NCs in formamide (FA, ε = 109), propylene carbonate (PC, ε = 65), DMSO (ε = 46), *N*,*N*-dimethylacetamide (DMA, ε = 38), dimethylformamide (DMF, ε = 37), and hexamethylphosphoramide (HMPA, ε = 30) but not in alcohols (ε < 30) or amines (ε < 10).

PbS−CdS NCs (sample **I**) exhibited bright PL in all of the above-mentioned solvents (QY ≈ 10−20%) with very similar

dx.doi.org/10.1021/ja2087689 | *J. Am. Chem.Soc.* 2012, 134, 2457−2460

steady-state PL spectra and PL lifetimes in the range 0.9−1.25 μs. The PL properties are also remarkably similar for fresh and 6-month-old samples stored under ambient conditions (Figure S8). We also prepared solutions of AsS_3^{3-}-capped NCs in tetrachloroethylene (TCE) by cation encapsulation with dodecyldimethylammonium ions (DDA^+).[14a] The observed decay times of 1.46 μs were longer than in all polar solvents and only slightly (<8%) shorter than for the original oleate-capped NCs in the same solvent (Figure 2B), pointing to a very minor effect of the inorganic capping on the exciton radiative recombination dynamics.

For low-temperature solution-based deposition of the a-As_2S_3 matrix, we adopted the method proposed by Chern and Lauks,[18] in which bulk As_2S_3 is dissolved in PA at room temperature to form highly concentrated solutions (typically 0.1−0.2 g/mL). Such liquid precursors have been used to fabricate inverse photonic crystals[19] and low-loss planar waveguides[12] and as inorganic photoresists.[18,20] It has been proposed that As_2S_3 breaks into small clusters (1−4 nm) capped with S^{2-} ions charge-balanced with alkylammonium cations.[21] The DLS data indeed pointed to such small species (Figure 3A, dilute solution).

Despite the low dielectric constant of PA (ε = 5.1), isolated PbS−CdS/AsS_3^{3-} NCs (d < 7 nm) are highly soluble in concentrated As_2S_3/PA solution (0.1−0.2 g mL^{-1} As_2S_3, 20−60 mg mL^{-1} NCs) but not in dilute solutions or neat PA. At the same time, the very small electrophoretic mobilities exclude purely electrostatic stabilization. For larger PbS−CdS NCs (d > 7 nm), the addition of 10−20 vol % DMSO was necessary to prepare stable colloids. Thus, colloidal stabilization of PbS−CdS NCs in As_2S_3/PA solutions occurred through simultaneous electrostatic and steric mechanisms. Because of the high As_2S_3 content, the DLS curves of NC dispersions closely matched those of the As_2S_3/PA solution (Figures 3A and S9).

Typically, spin-coating of concentrated As_2S_3/PA or PbS−CdS/As_2S_3/PA solutions at 3000 rpm onto hydrophilized glass, silicon, or silica substrates produced ∼1 μm thick homogeneous films (Figure 4). Precursor decomposition and removal of organic moieties occurred upon stepwise annealing under vacuum: 1 h at 60 °C, 1 h at 90 °C, and 1 h at 130 °C. Notably, $(NH_4)_3AsS_3$ completely decomposed at 100 °C, as revealed by thermogravimetric analysis (Figure S10). Several micrometer thick As_2S_3 films showed negligible absorption from C−H or N−H stretches (Figure S11), consistent with previous reports.[10,12,22] Importantly, solvent was removed well below the glass transition temperature (T_g = 185 °C). The amorphous nature of the matrix was confirmed by PXRD. As previously demonstrated,[10,22,23] the stoichiometry of as-deposited films is approximated as $As_2S_{3+x}(C_3H_7NH_3)_{2x}$. The low-temperature annealing generates hydrogenated arsenic sulfide, $As_2S_{3+x}H_{2x}$, followed by removal of hydrogen and excess sulfur (as H_2S) at higher temperatures.

Optically smooth, ∼1 μm thick films of PbS−CdS/As_2S_3 deposited onto SiO_2 substrates exhibited high transmittance in the IR spectral region with multiple interference fringes (Figure 4A) and very small scattering losses. This high optical quality allowed the film thickness and refractive index (n = 2.25 at λ = 1200 nm) to be determined using Swanepoel's method[24,25] in the transparent region. The As_2S_3 optical band gap of 2.15 eV, observed as an absorption edge at ∼500 nm (Figure 4A), was determined using Tauc's extrapolation from the plot of $(\alpha h\nu)^2$ against $h\nu$ in the high-absorption region (2−2.8 eV). To record optical absorption of PbS−CdS NCs in an As_2S_3 matrix in the absence of interference fringes, we prepared optically inhomogeneous films using partially destabilized colloids with additional PA and collected transmittance and total reflectance spectra using an integrating sphere (Figure S12). The resulting NC absorption spectrum showed excitonic absorption features at the same wavelengths as the original colloidal solutions, indicating that the NC materials endured the processing steps intact. Most importantly, we observed intense PL from the inorganic composites after the 130 °C annealing (Figure 4B).

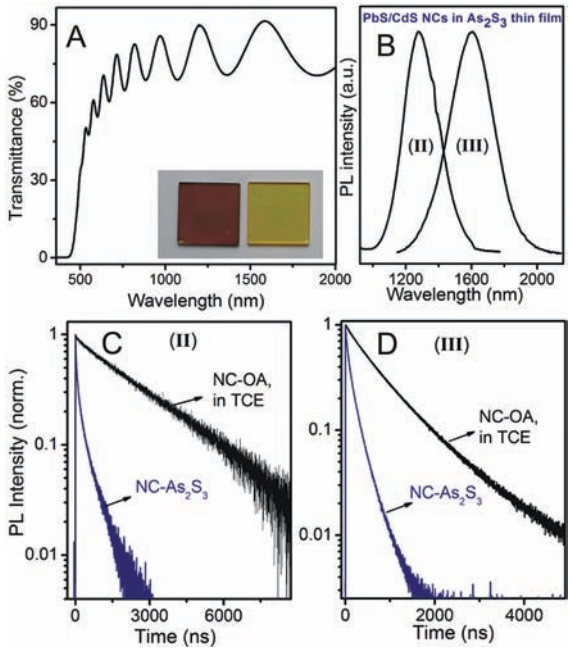

Figure 4. (A) Optical transmission and (B) PL spectra from PbS−CdS NCs (sample **II**) in an As_2S_3 thin film (∼1 vol % NCs) spin-coated onto 1 in.^{2} SiO_2 substrates. The inset in (A) shows photographs of ∼1 μm thick As_2S_3 films (brown) with ∼10 vol % and (yellow) without NCs. (C, D) Room-temperature time-resolved PL recorded at the emission-peak maxima for PbS−CdS NCs (samples **II** and **III**) in the indicated dielectric environments. The radiative lifetime of the NCs in the high-dielectric-environment matrix leads to a reduced PL lifetime in correspondence with estimates from dielectric screening.

The integration of lead chalcogenide NCs into an As_2S_3 matrix can help to overcome the very long T_r in lead chalcogenide NCs.[26−28] Relative to II−VI NCs ($T_r \approx$ 20 ns), PbS NCs show ∼2 orders of magnitude longer T_r .[26] Under optimal excitation conditions, the number of photons emitted by each NC per second is inversely proportional to T_r, and as a result, II−VI NCs can provide much brigher PL. Such long lifetimes in IV−VI NCs have induced earlier researchers to consider carrier trapping, exciton fine structure with spin-forbidden exciton character,[26] and the impact of dielectric screening.[26−28] We can use the high-refractive-index environment of the As_2S_3 matrix to provide insight to the origin of the unusually long radiative lifetime in lead chalcogenide NCs.

According to Wehrenberg et al.,[27] the radiative rate for lead chalcogenide NCs can be expressed as

$$T_r^{-1} = \left(\frac{3\varepsilon_1}{\varepsilon_2 + 2\varepsilon_1}\right)^2 \frac{2\gamma e^2 \sqrt{\varepsilon_1}\,\omega^2 f}{3{m_0}^2 c^3} \quad (1)$$

where ω is the photon frequency, e is the electron charge, m_0 is the free mass of the electron, c is the speed of light, f is the oscillator strength of the first exciton, and ε_1 and ε_2 are the

dx.doi.org/10.1021/ja2087689 | J. Am. Chem.Soc. 2012, 134, 2457−2460

optical dielectric constants of the solvent (or host) and semiconductor, respectively. Liu and Guyot-Sionnest[9] used $\gamma = {}^{3}/_{16}$ to account for the exciton degeneracy in structurally similar PbSe NCs. For PbS, $\varepsilon_2 \approx 17$, and eq 1 predicts that dielectric screening should result in a 10−12-fold increase in T_r for PbS NCs in typical nonpolar organic solvents or polymer matrices ($\varepsilon_1 \approx 2.0$−2.3) due to attenuation of the electric field inside the NCs.[27] Previous attempts to test this important hypothesis have proven inconclusive because of small variations in the ε_1 values for suitable solvents.[26] For our solution-processed As_2S_3 films, $\varepsilon_1 \approx 5.1$ was calculated from the measured refractive index. Such a high ε_1 value should lead to a significant reduction of the dielectric contrast. Upon examination of time-resolved data for PbS−CdS/As_2S_3 films, the decays clearly did not appear to be single-exponential. The fastest decay components typically arise from nonradiative processes, whereas the longest-lived exponential decay likely represents the intrinsic radiative process in NCs. For the PL decays in Figure 4C, the longest fitted lifetime of ∼530 ns was obtained for PbS−CdS NCs in an As_2S_3 matrix, which compares with a similarly fitted lifetime of 2600 ns for the same NCs dispersed in TCE ($\varepsilon_1 = 2.25$). The latter comparison yields a 4.9-fold difference in lifetime, in close agreement with the 4.83-fold difference predicted by eq 1. For PbS−CdS NCs with an emission peak at 1600 nm (sample **III**; Figure 4D), such an analysis gives a ratio of long-lived decay components of ∼4.1, again with shorter lifetimes observed for NCs in the As_2S_3 matrix. The similarity of the estimated differences in radiative lifetimes measured for the PL decay components suggests that dielectric screening does indeed heavily impact T_r for lead chalcogenide NCs.

In summary, we have shown that inorganically capped colloidal NCs can be combined with a-As_2S_3 to integrate the NCs into a chalcogenide glass host. Low-temperature integration of IR-emitting NCs into an IR-transparent inorganic matrix is an important step for optical and optoelectronic applications of colloidal NCs. This approach will be especially useful for NCs emitting in the mid-IR region,[6,8] where only a few host materials can provide good optical transparency. Among them, chalcogenide glasses are rather unique because of their very low phonon energies and low T_g, which are advantageous for making fibers and other optical elements. Our preliminary experiments have shown that the developed chemistry can be extended to different luminescent quantum dots (e.g., CdSe−ZnS), different inorganic capping ions (e.g., S^{2-}, SnS_4^{4-}), and different host materials (e.g., GeS_2). Furthermore, the large optical dielectric constant of a-As_2S_3 reduced the dielectric contrast between the NCs and the surrounding medium. Our data suggest that the high dielectric constant of the As_2S_3 medium permits fast radiative rates in otherwise "slow" PbS NCs.

■ ASSOCIATED CONTENT

Ⓢ Supporting Information

Experimental details and supporting figures. This material is available free of charge via the Internet at http://pubs.acs.org.

■ AUTHOR INFORMATION

Corresponding Author

mvkovalenko@ethz.ch; dvtalapin@uchicago.edu

Present Address

[⊥]Department of Chemistry and Applied Biosciences, ETH Zürich, CH-8093 Zürich, Switzerland, and EMPA-Swiss Federal Laboratories for Materials Science and Technology, CH-8600 Dübendorf, Switzerland.

■ ACKNOWLEDGMENTS

D.V.T. acknowledges support from NSF CAREER (DMR-0847535) and DOD ONR (N00014-10-1-0190). R.D.S. and D.V.T. acknowledge support by the University of Chicago and the U.S. DOE (section H.35 of Contract DE-AC02-06CH11357). Use of the Center for Nanoscale Materials was supported by DOE BES (Contract DE-AC02-06CH11357).

■ REFERENCES

(1) Murray, C. B.; Kagan, C. R.; Bawendi, M. G. *Annu. Rev. Mater. Sci.* **2000**, *30*, 545.
(2) Yin, Y.; Alivisatos, A. P. *Nature* **2005**, *437*, 664.
(3) Steckel, J. S.; Zimmer, J. P.; Coe-Sullivan, S.; Stott, N. E.; Bulovi, V.; Bawendi, M. G. *Angew. Chem., Int. Ed.* **2004**, *43*, 2154.
(4) Zimmer, J. P.; Kim, S.-W.; Ohnishi, S.; Tanaka, E.; Frangioni, J. V.; Bawendi, M. G. *J. Am. Chem. Soc.* **2006**, *128*, 2526.
(5) Talapin, D. V.; Lee, J. S.; Kovalenko, M. V.; Shevchenko, E. V. *Chem. Rev.* **2010**, *110*, 389.
(6) Pietryga, J. M.; Schaller, R. D.; Werder, D.; Stewart, M. H.; Klimov, V. I.; Hollingsworth, J. A. *J. Am. Chem. Soc.* **2004**, *126*, 11752.
(7) Rogach, A. L.; Eychmuller, A.; Hickey, S. G.; Kershaw, S. V. *Small* **2007**, *3*, 536.
(8) Kovalenko, M. V.; Kaufmann, E.; Pachinger, D.; Roither, J.; Huber, M.; Stangl, J.; Hesser, G.; Schaffler, F.; Heiss, W. *J. Am. Chem. Soc.* **2006**, *128*, 3516.
(9) Liu, H.; Guyot-Sionnest, P. *J. Phys. Chem. C.* **2010**, *114*, 14860.
(10) Song, S. S.; Dua, J.; Arnold, C. B. *Opt. Express* **2010**, *18*, 5472.
(11) Kohoutek, T.; Orava, J.; Prikryl, J.; Wagner, T.; Frumar, M. *J. Non-Cryst. Solids* **2011**, *357*, 157.
(12) Tsay, C.; Mujagic, E.; Madsen, C. K.; Gmachl, C. F.; Arnold, C. B. *Opt. Express* **2010**, *18*, 15523.
(13) Pietryga, J. M.; Werder, D. J.; Williams, D. J.; Casson, J. L.; Schaller, R. D.; Klimov, V. I.; Hollingsworth, J. A. *J. Am. Chem. Soc.* **2008**, *130*, 4879.
(14) (a) Kovalenko, M. V.; Bodnarchuk, M. I.; Talapin, D. V. *J. Am. Chem. Soc.* **2010**, *132*, 15124. (b) Kovalenko, M. V.; Bodnarchuk, M. I.; Zaumseil, J.; Lee, J. S.; Talapin, D. V. *J. Am. Chem. Soc.* **2010**, *132*, 10085. (c) Kovalenko, M. V.; Scheele, M.; Talapin, D. V. *Science* **2009**, *324*, 1417.
(15) Musikhin, S. F.; Bakueva, L. G.; Il'in, V. I.; Rabizo, O. V.; Sharonova, L. V. *Superlattices Microstruct.* **1994**, *15*, 495.
(16) Wuister, S. F.; Donega, C. D.; Meijerink, A. *J. Phys. Chem. B* **2004**, *108*, 17393.
(17) O'Brien, R. W.; White, L. R. *J. Chem. Soc., Faraday Trans.* **1978**, *74*, 1607.
(18) Chern, G. C.; Lauks, I. *J. Appl. Phys.* **1982**, *53*, 6979.
(19) Kohoutek, T.; Orava, J.; Sawada, T.; Fudouzi, H. *J. Colloid Interface Sci.* **2011**, *353*, 454.
(20) Hajto, E.; Belford, R. E.; Ewen, P. J. S.; Owen, A. E. *J. Non-Cryst. Solids* **1989**, *115*, 129.
(21) Kohoutek, T.; Wagner, T.; Frumar, M.; Chrissanthopoulos, A.; Kostadinova, O.; Yannopoulos, S. N. *J. Appl. Phys.* **2008**, *103*, No. 063511.
(22) Chern, G. C.; Lauks, I.; McGhie, A. R. *J. Appl. Phys.* **1983**, *54*, 4596.
(23) Chern, G. C.; Lauks, I. *J. Appl. Phys.* **1983**, *54*, 2701.
(24) Marquez, E.; Ramirez-Malo, J.; Villares, P.; Jimenez-Garay, R.; Ewen, P. J. S.; Owen, A. E. *J. Phys. D: Appl. Phys* **1992**, *25*, 535.
(25) Swanepoel, R. *J. Phys. E: Sci. Instrum.* **1983**, *16*, 1214.
(26) Clark, S. W.; Harbold, J. M.; Wise, F. W. *J. Phys. Chem. C* **2007**, *111*, 7302.
(27) Wehrenberg, B. L.; Wang, C.; Guyot-Sionnest, P. *J. Phys. Chem. B* **2002**, *106*, 10634.
(28) Du, H.; Chen, C.; Krishnan, R.; Krauss, T. D.; Harbold, J. M.; Wise, F. W.; Thomas, M. G.; Silcox, J. *Nano Lett.* **2002**, *2*, 1321.